Available online at www.sciencedirect.com
ScienceDirect
Chemometrics and Intelligent Laboratory Systems 84 (2006) 119–125
Chemometrics and intelligent laboratory systems
www.elsevier.com/locate/chemolab

Generalized correlation loadings
Extending correlation loadings to congruence and to multi-way models

G. Lorho [a,*], F. Westad [b], R. Bro [c]

[a] *Nokia Corporation, Finland*
[b] *The Norwegian Food Research Institute, Norway*
[c] *The Royal Veterinary and Agricultural University, Denmark*

Received 16 January 2006; received in revised form 6 April 2006; accepted 21 April 2006
Available online 14 July 2006

Abstract

Correlation loadings are commonly used in bi-linear models to highlight relationships between the original variables of a dataset and the latent variables resulting from the model. This principle is suggested to be renamed *congruence loading* and is extended to multi-way models. Congruence is proposed as a more meaningful parameter covering the case of centered data, as originally proposed with the correlation loading principle, but also the cases where data are not centered or centered across a different mode. The idea of congruence loadings is also extended to multi-way models, i.e. parallel factor analysis (PARAFAC), Tucker, and *N*-way partial least squares (*N*-PLS). In this paper, the method is applied to three-way models where the scores and/or loadings are not orthogonal. Three real datasets are considered to highlight some applications of congruence loadings. In the first example, a three-way sensory profiling dataset (assessors × products × attributes) is considered to illustrate the use of congruence loadings in exploratory data analysis with principal component analysis (PCA) and PARAFAC models. The second example concerns the ^{1}H NMR spectroscopy of a typical metabonomic dataset and shows how congruence loadings of a PARAFAC model makes it easier to visualize minor features in the data. The last example illustrates the use of congruence loadings for variable selection in PARAFAC-based curve-resolution of fluorescence data.

Keywords: Correlation loadings; Congruence; PARAFAC; Tucker; *N*-PLS; Sensory profiling data; ^{1}H NMR spectroscopy; Multivariate curve-resolution

1. Introduction

The development of advanced multivariate data analysis and the recent availability of different multi-way models in mathematical software packages, e.g. Matlab (The Mathworks), have favored the application of these analysis tools for data visualization, process optimization or calibration problems in different fields of research including chemometrics [1–3], food science [4,5] and digital signal processing [6]. The validation and interpretation of models are two important aspects of multivariate data analysis. Several methods have been presented in the literature for multi-way model validation, e.g. the bootstrap [7], jackknife [8], split-half [9] or concordia [10] methods. Model interpretation can include issues such as understanding the importance of variables in each mode of a model, identifying model components, or detecting outliers. Graphical techniques as found in two-way analysis are available for multi-way model visualization and interpretation. For example, the score and loading plots or the biplot [11] commonly found in bi-linear applications can be used in multi-way analysis. Another method referred to as *correlation loadings* has shown its usefulness in PCA and PLS applications [12,13]. In this paper, an extension of this correlation loading principle to multi-way models is proposed. The mathematical details concerning correlation and congruence loadings are presented for the two-way and multi-way cases in Section 2. Section 3 describes briefly the three datasets employed in this study. In Section 4, the principle of congruence loadings is applied to these three datasets and results regarding the relevance of this parameter are discussed.

* Corresponding author.
E-mail address: gaetan.lorho@nokia.com (G. Lorho).

0169-7439/$ - see front matter © 2006 Elsevier B.V. All rights reserved.
doi:10.1016/j.chemolab.2006.04.023

2. Background

2.1. Two-way theory

Bi-linear models are usually summarized with graphical tools, i.e. two-dimensional plots for scores and loadings to visualize the relations between samples and variables respectively along two components of the model. Biplots can also be employed to present both samples and variables on the same graph, which can improve model interpretability. The assessment of variable significance is an important aspect of bi-linear models. As reported in [13], 'rules of thumb such as a cut-off for loadings at values higher than, e.g. 0.3' can be used in PCA models. However, as the loading vectors have norm=1 in our data-analytical tradition, the effective range of values in a loading plot depends on the number of variables. Correlation loading plots, also referred to as *correlation circles*, can be employed to gain more insight to the data structure and to help model interpretability, regardless of the number of variables in the model. This method offers a scale-invariant presentation of variables, useful especially in cases where variables with different numerical ranges are present [12]. This type of plots indicates correlations between the original variables and the latent variables resulting from the model. Circles are often included in these plots to indicate 100% modeled variance, because the squared sum of the correlation loading co-ordinates for a given variable represents the variance explained by this variable. Therefore, the closer a variable is to the circle, the more important it is to explain the differences observed between the samples.

Mathematically, the correlation loading replaces the actual loading element of variable i, p_{if} with the correlation between the **centered** data at variable i, $\mathbf{x}_i$ and the specified latent variable $\mathbf{t}_f$ (PC #f). This parameter can therefore be expressed as a conventional *correlation coefficient*:

$$r_{if} = \mathrm{corr}\left(\mathbf{x}_i, \mathbf{t}_f\right) = \frac{\mathbf{x}_i^{\mathrm{T}}\mathbf{t}_f}{\sqrt{\left(\mathbf{x}_i^{\mathrm{T}}\mathbf{x}_i\right)\left(\mathbf{t}_f^{\mathrm{T}}\mathbf{t}_f\right)}} \tag{1}$$

As the loading p_{if} is defined as $p_{if}=\left(\mathbf{x}_i^{\mathrm{T}}\mathbf{t}_f\right)/\left(\mathbf{t}_f^{\mathrm{T}}\mathbf{t}_f\right)$, another expression for the correlation loading can be derived as follows:

$$r_{if} = \frac{\left(\mathbf{x}_i^{\mathrm{T}}\mathbf{t}_f\right)\mathbf{t}_f^{\mathrm{T}}\mathbf{t}_f}{\mathbf{t}_f^{\mathrm{T}}\mathbf{t}_f\sqrt{\left(\mathbf{x}_i^{\mathrm{T}}\mathbf{x}_i\right)\left(\mathbf{t}_f^{\mathrm{T}}\mathbf{t}_f\right)}} = p_{if}\frac{\mathbf{t}_f^{\mathrm{T}}\mathbf{t}_f}{\sqrt{\left(\mathbf{x}_i^{\mathrm{T}}\mathbf{x}_i\right)\left(\mathbf{t}_f^{\mathrm{T}}\mathbf{t}_f\right)}} = p_{if}\frac{\sqrt{\mathbf{t}_f^{\mathrm{T}}\mathbf{t}_f}}{\sqrt{\mathbf{x}_i^{\mathrm{T}}\mathbf{x}_i}} \tag{2}$$

which is the formula usually presented.

A similar correlation loading approach can be employed for PLS models [14]. Both X- and Y-variables can be represented by their correlation loadings in this case. The Eq. (1) can be applied to compute the correlation loadings of the Y-variables, with $\mathbf{Y}$ corresponding to a vector in the case of a PLS-1 model, and to a matrix in the PLS-2 case. Due to the scale-invariant representation of the variables, correlation loadings of $\mathbf{X}$ and $\mathbf{Y}$ can be displayed on the same plot and assessed based on their position on the circle of correlations.

2.2. A new name: congruence loading

Correlation loading is the name attached to the above modified loadings. However, for models that do not employ centering of the data, such correlation-based loadings are not meaningful. Correlation between a loading and a variable is meaningful for centered data because the correlation is directly related to the variance explained of the centered data. If the data are uncentered or centered across another mode, then congruence is a more meaningful parameter. For centered data, congruence and correlation are equivalent. For uncentered data, correlation is not at all related to the variation explained because the correlation specifically disregards the offset which is not actually removed from the data. Congruence on the other hand is the similarity between the uncentered entities and so directly reflects the variation explained.

2.3. Multi-way theory

Multi-way models such as PARAFAC, TUCKER or N-PLS are also commonly summarized with graphical tools, e.g. a score plots highlighting the relations between samples and a set of loading plots for each variable in the case of a PARAFAC model. As visualization of important variables in each mode can sometimes be difficult with these models, an analogy to the two-way correlation loading plot idea was considered and a generalization to the multi-way case was developed in this study, as presented next.

Only three-way models are considered explicitly, but it will be evident that the approach suggested extends in a simple manner to any order. Firstly, note that for multi-way analysis, it is common practice not to distinguish between scores and loadings. Rather they are all referred to as *loading*. This also indicates that congruence loadings can actually be derived for any mode desired. This is even possible in the above two-way case. In order to derive congruence loadings for multi-way models consider algebraic expressions for PARAFAC and Tucker models [15], for a given three-way array $\underline{\mathbf{X}}$ ($I\times J\times K$)

$$\text{PARAFAC} \quad \mathbf{X} = \mathbf{A}(\mathbf{C}\odot\mathbf{B})^{\mathrm{T}}+\mathbf{E} \tag{3}$$

$$\text{Tucker} \quad \mathbf{X} = \mathbf{A}\mathbf{G}(\mathbf{C}\otimes\mathbf{B})^{\mathrm{T}}+\mathbf{E} \tag{4}$$

Above, $\mathbf{X}$ is the matricized array of size $I\times JK$ and likewise $\mathbf{G}$ is the matricized core array. The underlying model in N-PLS is the same as the Tucker model, which is therefore implicitly covered by the above. In both cases above, the model expressed in terms of matricized arrays can be written as a bilinear model $\mathbf{X}=\mathbf{A}\mathbf{Z}^{\mathrm{T}}+\mathbf{E}$ where the content of $\mathbf{Z}$ is given by Eqs. (3) and (4). The matrix $\mathbf{Z}$ can easily hold the corresponding loadings of a four-way, five-way, etc., model as shown e.g. in [16] and hence this expression is generally valid for multi-way models. To derive congruence loadings for the first mode, simply let the element r_{if} be defined as the congruence between the vectorized ith slab of $\bar{\mathbf{X}}$, $\mathbf{X}_i$, and the vector $\mathbf{z}_f$. Some computational shortcuts are possible taking the structure of the model into account. For example, for the first mode loadings in a

PARAFAC model, the correlation loadings are defined as follows, letting **b** and **c** be the *f*th column of **B** and **C**, respectively:

$$\text{congruence}\left(\text{vec}\mathbf{Z}_f, \text{vec}\mathbf{X}_i\right) = \frac{\mathbf{b}^{\mathrm{T}}\mathbf{X}_i\mathbf{c}}{\sqrt{\left(\mathbf{b}^{\mathrm{T}}\mathbf{b}\right)\left(\mathbf{c}^{\mathrm{T}}\mathbf{c}\right)\left(\text{vec}\mathbf{X}_i^{\mathrm{T}}\,\text{vec}\mathbf{X}_i\right)}} \quad (5)$$

For models in which the loadings in **Z** are not orthogonal, the variation explained by two components is not additive, hence they may even sum to more than 100%. This mostly holds for PARAFAC but also for two-way multivariate curve-resolution solutions. In such cases, it is not meaningful to draw circles in congruence loading plots as they do not imply 100% explained variance. Rather, each component has to be assessed individually. In order to signify this, plots are shown with squares rather than circles.

3. Experimental

Three real datasets are considered in this paper to illustrate the relevance of congruence loadings in different applications including sensory profiling of food products, ^{1}H nuclear magnetic resonance of carbohydrates, and fluorescence excitation–emission spectroscopy of chemical analytes. Data used in this paper comes from the literature and the reader is referred to this earlier literature for details on the data.

3.1. Sensory profiling data

The sensory dataset analyzed in this paper originates from a study by Folkenberg et al. [17] in which cocoa-milk products were evaluated in three replicates by a panel of assessors using a set of consensus sensory attributes. Data averaging over replicates gave a three-way array of size 7 × 15 × 15 (assessors × products × attributes). However, 25% of artificial variables, referred to as *random* in the following section, was added to the cocoa dataset for the present study, i.e. one variable in each mode, leading to a 8 × 16 × 16 array. These data consisting of columns of random numbers selected on a magnitude scale of the original data scale was added to illustrate the effect of noisy data on congruence loadings in the different models. This three-way dataset was preprocessed by centering across products and scaling within subjects prior to PARAFAC modeling (see [18] for a formal description of multi-way array normalization). The two-way dataset for the PCA model was obtained by averaging the preprocessed three-way array over assessors.

3.2. ^{1}H nuclear magnetic resonance data

The ^{1}H NMR dataset employed here is similar to the study by Bro et al. [19] but with slightly different analytes. Mixtures of glucose, maltose and maltotriose were made according to a reduced three-level design. Only eight samples were used for modeling. These samples were prepared with the three compounds at 0, 10 and 20 mM. The compounds were dissolved in a pH 6.0 phosphate buffer (0.1 M) in D_2O. The samples were prepared as 500 μl of the above described solutions with 50 μl 1 mg/ml TSP (3-trimethylsilyl-1-[2,2,3,3-2*H*4] propionate) in D_2O added as chemical shift reference (0.0 ppm). Proton spectra were measured at 298 K on a Bruker DRX600 operating at 14.1 T using a flow-NMR system and a 120 μl flow-probe. The pulse program used was a stimulated echo experiment with bipolar gradient pulses and a longitudinal eddy current delay as well as pre-saturation to suppress residual H_2O signal. The gradient was varied in 32 steps from 0.05 to 0.95 of maximum gradient power using a squared ramp.

3.3. Fluorescence data

An example of fluorescence excitation–emission spectroscopy is presented in which a PARAFAC model is employed to estimate relative concentrations and pure analyte spectra from fluorescence measurements of chemical analytes in mixtures. Twenty-seven synthetic samples containing different concentrations of four analytes (hydroquinone, tryptophan, phenylalanine and dopa) were measured in a Perkin-Elmer LS50 B fluorescence spectrometer. Each fluorescence landscape originally consists of 551 emission wavelengths (200–610 nm) and 24 excitation wavelengths (200–315 nm taken each 5 nm intervals). More details about this study can be found in, e.g. [20,8,16].

4. Results and discussion

4.1. Exploratory analysis of sensory profiling data

4.1.1. Two-way analysis

A PCA model was applied to the two-way average sensory profiling dataset to explore the systematic structure of the data. Fig. 1 illustrates the two first components, which explain 78.9% of the variation in the data. The score and loading plots (upper graphs) represent respectively the score of each sample and the loading of each variable along the two first principal components. The sample separation seen along the second latent variable is due to the presence or not of a stabilizer in the cocoa drink composition as described in [17]. It can be noted from the upper graphs of Fig. 1 that the artificial sample and variable consisting of random numbers are not clearly separated from the real variables, e.g. the attribute *mouthfeel* shows as low loading values as the random variable. The principle of congruence was applied to both scores and loadings in this example (lower graphs in Fig. 1) to assess the relative importance of variables in the model. From these congruence loading plots, we can see a clearer separation between the random data and the other samples and variables. Most of the products are well described by the first two components of the model (closeness to the outer circle on the lower-left graph), except the sample #14 lying inside the inner circle (50% explained variance). Few variables also show a lower explained variance level than others, e.g. *bitter*, *balanced* and *mouthfeel* positioned close to the inner circle (lower-right graph).

It should be noted that congruence is equivalent to correlation for the attribute loadings due to the centering across

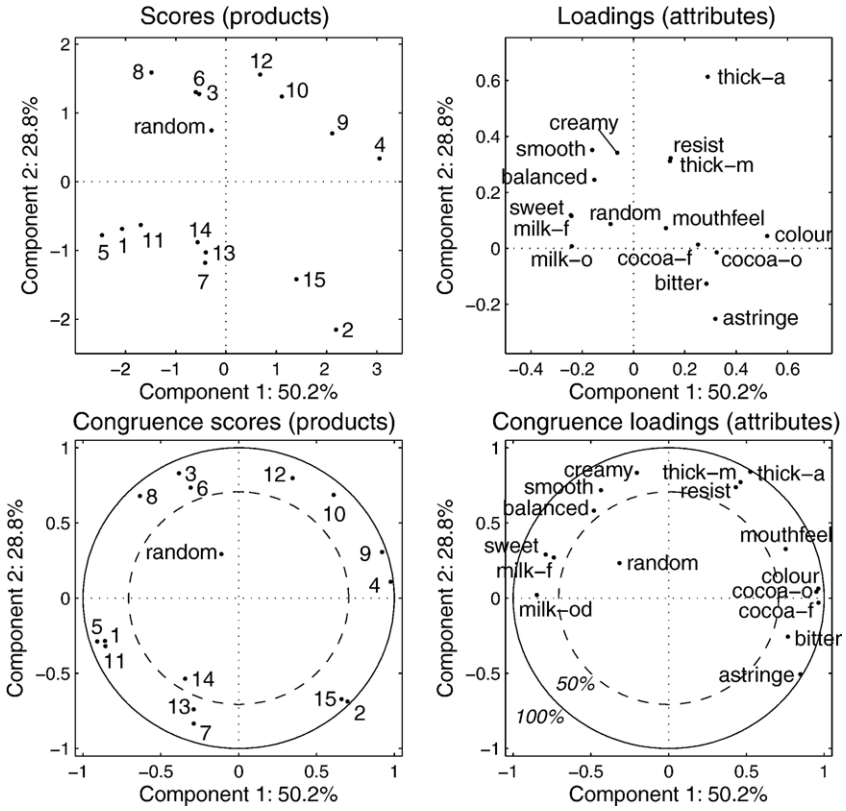

Fig. 1. Two-component PCA model of the sensory profiling dataset. Upper graphs: score and loading plots. Lower graphs: congruence plots for both scores and loadings. Outer (solid line) and inner (dashed line) circles represent, respectively, 50% and 100% additive explained variance.

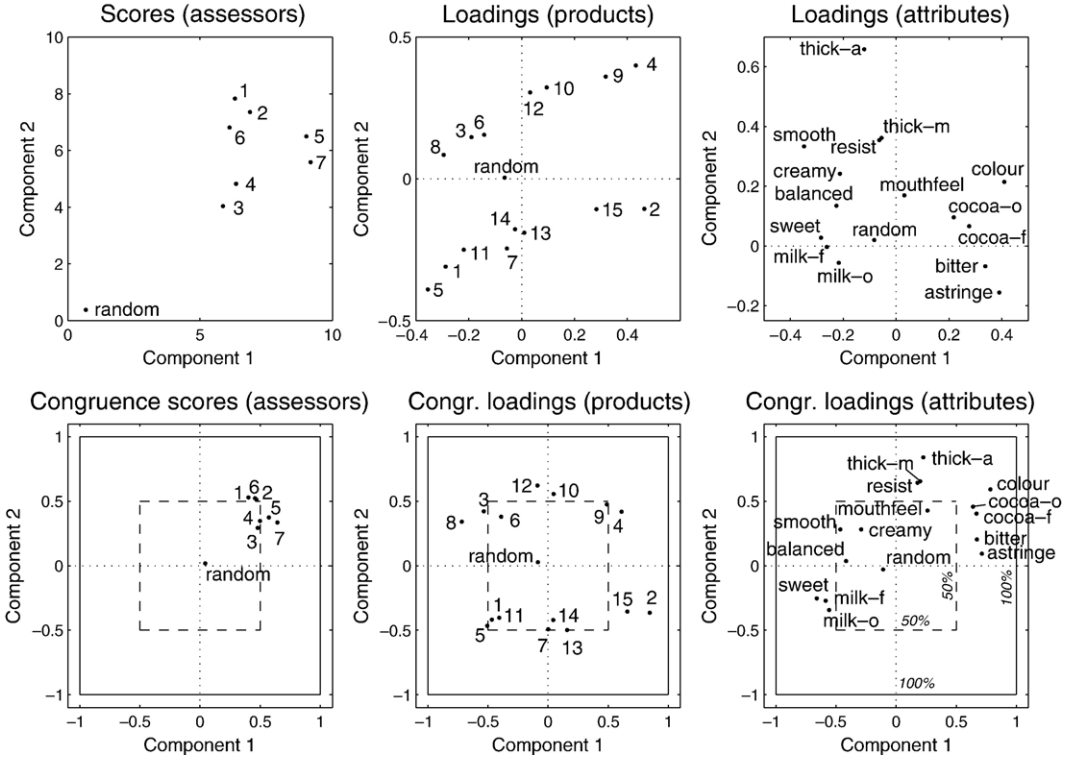

Fig. 2. Two-component PARAFAC model of the sensory profiling dataset. Upper graphs: score and loading plots. Lower graphs: congruence plots for each mode. Outer (solid line) and inner (dashed line) squares represent, respectively, 50% and 100% explained variance for each latent component separately.

products applied in the dataset pre-processing step. However, this is not the case for the PCA scores and applying the correlation loading principle to sample scores might result in sums superior to 1, i.e. samples positioned outside the 100% correlation circle.

4.1.2. Three-way analysis

The result of a two-component PARAFAC model applied to the sensory profiling dataset is presented in Fig. 2. The upper graphs include a score plot for assessors and two loading plots, i.e. one for products and one for attributes. The model explains only 41.8% of the variation in the data but it should be noted that a model showing similar patterns with a fit of 74.9% is obtained for the same dataset without the artificial variables. The product loading plot in this PARAFAC model (upper–middle graph, Fig. 2) shows a sample clustering similar to the PCA model (Fig. 1). In comparison to PCA, the scores of a PARAFAC model offer additional information about individual assessors. The artificial variables *random* do not contribute much to the model, as can be seen from their very low scores and loadings on both components (upper graphs in Fig. 2). However, assessing the relative importance of the attributes to the model is not straightforward from the attribute loading plot (upper–middle graph of Fig. 2).

Applying the congruence loading method to this model gives the result illustrated in the lower graphs of Fig. 2. Note the use of squares instead of circles in these plots to highlight the non-orthogonality of components in PARAFAC models. We see from these graphs that the random variables remain very close to the center in each congruence plot, whereas some attributes stand apart with a larger congruence loading value along one of the latent variables, e.g. *colour*, *bitter*, *astringe*, *cocoa-f* and *cocoa-o* for the first component, and *thick-a*, *thick-m*, *resist* and *colour* for the second component. However, a lower congruence loading value can be seen for the attributes *creamy*, *balanced*, *smooth* and *mouthfeel*. These attributes remain inside the inner rectangle representing 50% explained variance for each component, which means that they contribute less to the model. Based on the information obtained from this congruence loading plot, a more detailed analysis might be considered for these specific sensory attributes, e.g. assessing agreement between assessors or measuring average product discrimination.

4.2. Visualization of minor features in ^1H NMR data

In 2D diffusion-edited NMR the signal intensity is recorded as a function of chemical shift as well as of gradient strength:

$$I_{\delta gk} = \sum_{f=1}^{F} S_{\delta f} A_{gf} C_{kf} \tag{6}$$

where $S_{\delta f}$ denotes the spectral intensity at chemical shift δ for compound f, and where $A_{gf}=\exp(-D_f\gamma^2 g^2 \Delta' - R_f)$ denotes the attenuation due to diffusion (D_f) at gradient strength g for compound f, and C_{kf} denotes the concentration in sample k of compound f. When comparing the above model with a PARAFAC model, it follows that 2D diffusion-edited data can be separated into individual constituent spectra ($\mathbf{b}_f$), diffusion profiles ($\mathbf{c}_f$) and concentrations ($\mathbf{a}_f$) as was shown by Bro et al. [19].

Here an example of such a PARAFAC model is given (Fig. 3). In many e.g. metabonomic studies, one main purpose of the analysis is to be able to explore which peaks are present and which are absent in different components. This can be complicated because of large magnitude differences across the chemical shift axis. For these particular data there

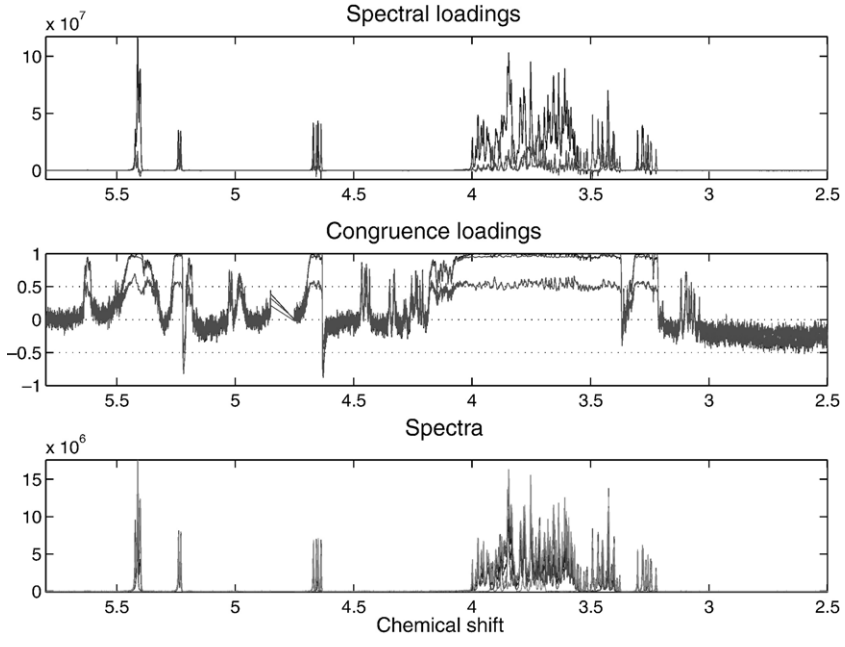

Fig. 3. PARAFAC model of ^1H NMR spectroscopy data: NMR spectra of the eight mixture samples used in this study (lower graph), PARAFAC loading spectra representing an estimate of the three compound spectra (upper graph) and associated correlation loadings (middle graph).

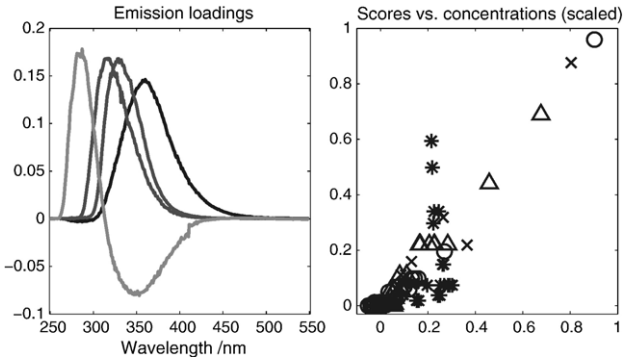

Fig. 4. Emission loading plot from a four-component PARAFAC model of the fluorescence data (left graph) and scatter plot of scores versus analyte concentrations in the samples (right graph).

are many peaks of varying size, and even the very minor peaks may be important to identify. A three-component PARAFAC model is appropriate for the 2D NMR data.

In the resulting loadings, several peaks are almost impossible to detect in both loadings and raw data. But in the congruence loadings these are easily spotted. This is e.g. evident around 5 ppm but also in several other places.

Upon detection in the congruence plot, these peaks are possible to detect in the loadings by zooming in on the right areas, but the detection of where to zoom in is very much simplified by the use of the congruence loadings. Note also, the interesting fact that some minor peaks are not at all visible in the raw data. Only when averaging over many samples as is essentially done in computing the loadings, can they be detected visually.

4.3. Variable selection in fluorescence data

This example shows how congruence loadings might be utilized for variable selection in PARAFAC-based curve-resolution of fluorescence data. The raw fluorescence data include several areas (mainly scattering areas) which can be immediately removed as it is known that these will merely disturb modeling of the sought chemical variation. Although the irrelevant variation has been removed, modeling is not straightforward. In theory, a four-component PARAFAC model should provide good estimates of underlying spectra and concentrations. Emission loadings and scatter plot of scores versus analyte concentrations in the samples are shown in Fig. 4. The negative loading and the bad correlations between scores and concentrations indicate that the model is not very good. Also, the PARAFAC only explains 95% of the variation which is less than expected for the type of data.

Looking at the congruence loadings of the model (Fig. 5), several interesting features are apparent. The low emission area seems irrelevant (very low congruence loadings for all components). This, however, was already apparent in the loadings or even in the raw data for that matter. More interesting is it that the low excitation areas are also seen to have fairly low congruence loadings for all components. This is not at all apparent from the loadings or the raw data. In fact, the excitation loadings in the low area are among the highest loadings. This shows that with a four-component model, this area is particularly poorly modeled and suggests that although the signal is high, it is not consistent with the model.

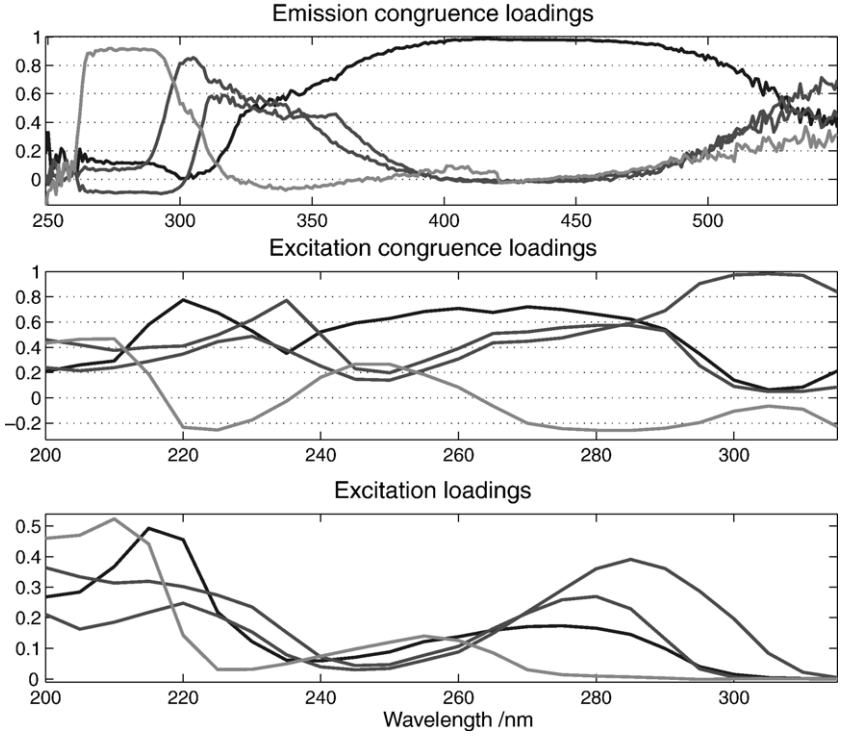

Fig. 5. Excitation loadings (lower graph), excitation congruence loadings (middle graph) and emission congruence loadings (upper graph) of a four-component PARAFAC model of the fluorescence data.

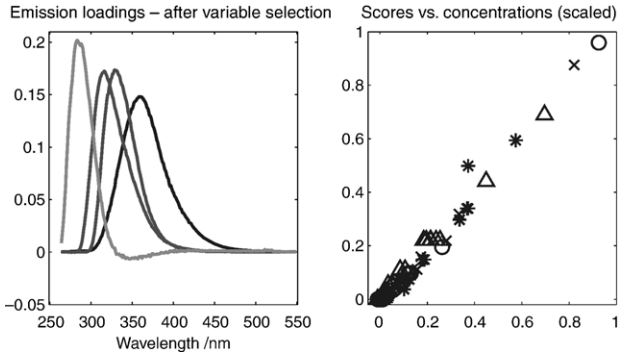

Fig. 6. Emission loading plot from a four-component PARAFAC model of fluorescence data with low-wavelengths removed (left graph) and scatter plot of scores versus analyte concentrations in the samples (right graph).

Subsequently, removing the two low-wavelength areas (excitation as well as emission) leads to a model with significantly improved characteristics. As can be observed in Fig. 6, emission loadings are now much more sensible and the scatter plot of scores versus concentrations shows the expected linear relation. Further elaboration of the model could be possible by making calibration models directly targeted towards only one specific chemical analyte, but this is not pursued here.

5. Conclusions

An extension of the principle of correlation loadings was proposed in this paper. In the context of multi-way analysis, the congruence between an original variable of a dataset and a latent variable resulting from the model is a more meaningful parameter than the correlation because it measures the similarity between uncentered entities and so directly reflects the variation explained. The idea of congruence loadings was extended to multi-way models where the scores and/or loadings are not necessarily orthogonal. Three real datasets were considered to highlight some applications of congruence loadings. The sensory profiling dataset example illustrated the use of congruence loadings in exploratory data analysis. Congruence loadings were applied to both two-way PCA and three-way PARAFAC models to show the link between the congruence loading plot and the original two-way correlation loading plot. However, the non-orthogonality of components in PARAFAC models implies that each component has to be assessed individually and to signify this, congruence loading plots were shown with squares rather than circles. In the second example, a ^{1}H NMR spectroscopy dataset was also employed to illustrate how congruence loadings of a PARAFAC model makes it easier to visualize minor features in the data. In this example, spectral peaks that were difficult to detect in both loadings and raw data turned out to be easily detected from the congruence loadings. Finally, a problem of variable selection in PARAFAC-based curve-resolution of fluorescence data was considered as a last example to illustrate the potential of congruence loadings for multi-way model improvement.

Acknowledgments

Part of the work reported in this paper was carried out during a visit of the first author to the Department of Dairy and Food Sciences, The Royal Veterinary and Agricultural University (KVL) in 2003/2004, which was sponsored by a scholarship from NorFA and from the LMC/MRI program (KVL). The authors would like to thank Ditte Folkenberg, Wender Bredie and Magni Martens for the use of the cocoa sensory profiling data from [17] in this study.

References

[1] R.G. Brereton, Analyst 125 (2000) 2125–2154.
[2] B.J. Prazen, K.J. Johnson, A. Weber, R.E. Synovec, Anal. Chem. 73 (2001) 5677–5682.
[3] R.D. Jiji, G.A. Cooper, K.S. Booksh, Anal. Chim. Acta 397 (1999) 61–72.
[4] R. Bro, H. Heimdal, Chemom. Intell. Lab. Syst. 34 (1996) 85–102.
[5] P.M. Brockhoff, D. Hirst, T. Næs, in: T. Næs, E. Risvik (Eds.), Multivariate Analysis of Data in Sensory Science, Elsevier, Amsterdam, 1996, pp. 307–342.
[6] N.D. Sidiropoulos, G.B. Giannakis, R. Bro, IEEE Trans. Signal Process. 48 (2000) 810–823.
[7] J. Kiers, J. Chemom. 18 (2004) 22–36.
[8] J. Riu, R. Bro, Chemom. Intell. Lab. Syst. 65 (2003) 35–49.
[9] R.A. Harshman, W.S. De Sarbo, in: H.G. Law, C.W. Snyder, J.A. Hattie, R. P. McDonald (Eds.), Research Methods for Multimode Data Analysis, Praeger Special Studies, New York, 1984, pp. 602–642.
[10] R. Bro, J. Kiers, J. Chemom. 17 (2003) 274–286.
[11] J.E. Jackson, A User's Guide to Principal Components, Wiley, New York, 1991.
[12] H. Martens, M. Martens, Multivariate Analysis of Quality. An Introduction, Wiley, Chichester, 2001.
[13] F. Westad, M. Hersleth, P. Lea, H. Martens, Food Qual. Prefer. 14 (2003) 463–472.
[14] H. Martens, M. Martens, Food Qual. Prefer. 11 (2000) 5–16.
[15] R. Bro, Doctoral Thesis: Multi-way analysis in the food industry. Models, algorithms, and applications, University of Amsterdam, 1998.
[16] A. Smilde, R. Bro, P. Gelati, Multi-Way Analysis. Applications in the Chemical Sciences, Wiley, Chichester, 2004.
[17] D. Folkenberg, W. Bredie, M. Martens, J. Sens. Stud. 14 (1999) 181–195.
[18] R. Bro, A.K. Smilde, J. Chemom. 17 (2003) 16–33.
[19] R. Bro, P.I. Hansen, N. Vierick, M. Dyrby, H.T. Pedersen, S.B. Engelsen, in: S.B. Engelsen, P.S. Belton, H.J. Jakobs (Eds.), Magnetic Resonance in Food Science. The Multivariate Challenge, The Royal Society of Chemistry, 2005, pp. 195–203.
[20] D. Bausgaard, Factors Affecting 3-Way Modelling (PARAFAC) of Fluorescence Landscapes, Royal Veterinary and Agricultural University, Department of Dairy and Food Science, Frederiksberg, Denmark, 1999.